Model Predictive Control for underactuated spacecraft equipped with two reaction wheels in the presence of a residual angular momentum

IAC–24–C1,1,x81182

Model Predictive Control for underactuated spacecraft equipped with two reaction wheels in the presence of a residual angular momentum

G. Avanzini[a*], E. de Angelis[b], F. Giulietti[b], C. Novara[c], M. Pagone[c]

[a]*Department of Engineering for Innovation, Università del Salento, 73100 Lecce, Italy*
{giulio.avanzini@unisalento.it}

[b]*Department of Industrial Engineering, Alma Mater Università di Bologna (Forlì Campus), 47121 Forlì, Italy*
{fabrizio.giulietti@unibo.it, emanuele.deangelis4@unibo.it}

[c]*Department of Electronics and Telecommunications, Politecnico di Torino, 10129 Turin, Italy*
{carlo.novara@polito.it, michele.pagone@polito.it}

[*] Corresponding Author.

Abstract

We propose a Nonlinear Model Predictive Control (NMPC) law for an underactuated spacecraft attitude maneuver in the presence of a momentum bias. We assume that a cluster of only two reaction wheels is available and the spacecraft is no longer fully controllable and stabilizable by means of a continuous static feedback. Nonlinear Model Predictive Control is investigated as a possible approach for the derivation of a suitable control system, which allows for full three-axis control, in spite of underactuation, with acceptable closed-loop performance, in the presence of a residual angular momentum and torque saturation. Maneuver convergence is studied and analyzed in two different scenarios: i) a minimum non-zero pointing error at rest condition; ii) a periodic spinning solution which allows a zero pointing error with a residual angular rate. An extensive simulation campaign shows the effectiveness of the proposed NMPC-based control, proofing the viability of the approach.

Keywords: Attitude control; underactuated spacecraft; nonlinear model predictive control; nonlinear systems

1. Introduction

Spacecraft (SC) attitude control is a challenging tasks, which can be successfully performed as far as the SC is equipped with actuators that can deliver a control torque along three mutually-independent directions (see, e.g., [1, 2, 3, 4] and references therein). This requires a minimum of three attitude actuators, such as thrusters, reaction wheels, magnetic torquers, etc [5]. Some degree of redundancy are required to maintain full spacecraft operability after failure of one of the actuators. In recent decades there has been an increasing interest in attitude control in underactuated conditions (see, e.g., [6]), when the number of available actuators can deliver only two independent torque components to control three rotational degrees of freedom. In such a case, the attitude stabilization becomes impossible by means of a continuous static feedback [7]. Hence, time-varying and/or switching control logics need to be envisaged to overcome this issue.

Attitude control of spacecraft in underactuated conditions thus represents a major challenge, relevant in practical operational mission scenarios after failure of one reaction wheel in a non-redundant three-wheel cluster, or multiple failures, when more than three reaction wheels are installed. If on one side many techniques based on switching control logics or time-varying controllers were proposed in the past, a general and closed solution to the problem is yet to be found. In two recent papers [8, 9] a control task simpler than exact attitude acquisition was investigated, that is, pointing of a body-fixed direction $\hat{\boldsymbol{\sigma}}$ towards a prescribed target direction $\hat{\boldsymbol{\tau}}$, fixed in the inertial frame, by means of a cluster of only two reaction wheels. In this framework, the angular position of the spacecraft around the target direction is not relevant, thus reducing the number of attitude variables to be controlled from three to two, which makes the control problem solvable by means of a reduced number of RWs. In [8] the total angular momentum of the spacecraft (platform and RWs) is assumed to be zero, and $\hat{\boldsymbol{\sigma}}$ can be aligned towards any arbitrary direction $\hat{\boldsymbol{\tau}}$, with zero residual angular speed. When a momentum bias $\boldsymbol{h}_0$ is present, the pointing maneuver is possible with a zero residual platform angular rate only if the plane identified by the spin axes of the two RWs can contain the (inertially fixed) direction of $\boldsymbol{h}_0$, posing a constraint on admissible pointing directions [9].

In the recent past, an approach based on Model Predictive Control (MPC) which can steer the spacecraft towards a prescribed attitude during large angle slew maneuvers as well as stabilize it by means of a cluster of only two reaction wheels (RWs) was successfully developed and widely tested in simulation in the ideal case of zero residual angular momentum [6]. Unfortunately, in a realistic operational scenario, the presence of environmental perturbing torques makes the assumption of zero angular momentum not always applicable. In this paper we take a step further by aiming at developing a MPC-based control technique which can handle such an issue. It should be noted that, in case a rest-to-rest maneuver is envisaged, the final attitude of the spacecraft is still constrained by the need of absorbing the residual angular momentum into the two active RWs. This means that an arbitrary desired attitude cannot, in general, be achieved, provided that the plane determined by the spin axes of the active RWs must contain the direction of the angular momentum. Note that, in the presence of environmental disturbance torque, this direction is not exactly constant in the inertial frame, but the timescale of its variation is sufficiently slow to be considered negligible with respect to the time required for performing the desired attitude maneuvers. Hence, over sufficiently short time intervals, $\boldsymbol{h}_0$ is assumed (at least approximately) constant in the inertial frame.

In this paper, two preliminary analytical results are initially derived. First, the admissible attitude which minimizes the error in terms of Euler angle rotation with respect to the desired one with the platform at rest is determined. Second, a spinning condition is determined, which forces the spacecraft to spin around the underactuated axis, thus achieving a smaller attitude error, although only for a fraction of the rotation. Two different MPC strategies are then proposed. In the first case, the minimum error attitude achievable by the SC with respect to the desired reference attitude is provided as a reference for the controller. In this case, the minimum attitude error can be asymptotically approached. A second strategy is analyzed for the spinning scenario, which allows the SC to pass closer to the target attitude, if compared to the minimum error attitude at rest determined above, but only for a limited amount of time, inversely proportional to the residual angular rate. During most of the resulting attitude motion, the pointing error becomes much larger.

Among several available control approaches for attitude control, MPC offers a framework where a control scheme with proven convergence capabilities becomes available, without exploiting specific physical properties of the system, thanks to its intrinsic nature, capable of dealing with complex (and possibly switching) systems [10]. MPC's success in SC attitude control bears the hallmark of generating optimal control signals for complex nonlinear systems, considering state, input, and output constraints [11, 12, 13]. In essence, MPC employs the a model of the dynamics to foresee future states and optimize control inputs within a finite time horizon. This dynamic adaptation capability enables spacecraft to be effectively robust with respect to evolving conditions and disturbances. Considering that the attitude kinematics and dynamics of spacecraft are highly nonlinear processes, a Nonlinear MPC (NMPC) approach is adopted in the paper [14].

2. Spacecraft model

2.1 *System dynamics*

Assuming that the spacecraft is rigid, a set of principal axes of inertia is selected as the body frame, $\mathcal{F}_B = \{G; \hat{\boldsymbol{e}}_1, \hat{\boldsymbol{e}}_2, \hat{\boldsymbol{e}}_3\}$, centered in the spacecraft center of mass, G. Unless otherwise stated, all vector quantities are represented in $\mathcal{F}_B$. When spacecraft attitude with respect to the inertial frame $\mathbb{F}_I$ is represented in terms of the unit quaternion [15] $\boldsymbol{q} = [q_0, q_1, q_2, q_3]^\top = [q_0, \bar{\boldsymbol{q}}^T]^\top$, the coordinate transformation matrix between $\mathcal{F}_I$ and $\mathcal{F}_B$ is

$$\mathbb{T}_{BI} = (q_0^2 - \bar{\boldsymbol{q}}^T\,\bar{\boldsymbol{q}})\boldsymbol{I}_3 + 2\bar{\boldsymbol{q}}\,\bar{\boldsymbol{q}}^T - 2q_0\,\bar{\boldsymbol{q}}^\times \qquad [1]$$

where $(\,\cdot\,)^\times$ denotes the skew–symmetric matrix equivalent to the cross product. The time derivative of the quaternion vector is

$$\dot{\boldsymbol{q}} = \frac{1}{2}\begin{bmatrix} -\bar{\boldsymbol{q}}^T \\ q_0\,\boldsymbol{I}_3 + \bar{\boldsymbol{q}}^\times \end{bmatrix}\boldsymbol{\omega}. \qquad [2]$$

where $\boldsymbol{\omega}$ is spacecraft angular velocity with respect to $\mathcal{F}_I$.

The total angular momentum of the spacecraft is

$$\boldsymbol{h} = \boldsymbol{J}\boldsymbol{\omega} + \boldsymbol{h}_r$$

where $\boldsymbol{J} = \mathrm{diag}(J_1, J_2, J_3)$ is the inertia tensor. Without loss of generality, we assume that the axis of the failed wheel is parallel to the third body axis, $\hat{\boldsymbol{b}} = \hat{\boldsymbol{e}}_3$, so that the relative angular momentum vector stored in the active reaction wheels is $\boldsymbol{h}_r = [h_1, h_2, 0]^\top$, with $h_i = I_w\Omega_i$, $i = 1, 2$, where I_w is wheel moment of inertia and Ω_i its rotation rate with respect to $\mathcal{F}_B$. Hence

$$\boldsymbol{h}_r = [h_{r_1},\, h_{r_2},\, 0]^\top = I_w \sum_{i=1}^{2} \Omega_i\,\hat{\boldsymbol{e}}_i \qquad [3]$$

The angular momentum balance equations are written in compact vector form as

$$\dot{\boldsymbol{\omega}} = \boldsymbol{J}^{-1}\,[\boldsymbol{M}_d - \boldsymbol{\omega}\times\boldsymbol{h}] \qquad [4]$$

where $\boldsymbol{M}_d$ is the external disturbance torque. Provided that the duration of the maneuver is limited, we assume

that the effect of $\boldsymbol{M}_d$ on the angular momentum is negligible over a sufficiently small time interval (that is, $\boldsymbol{M}_d \approx \boldsymbol{0}$), and the angular momentum vector

$$\boldsymbol{h}_I = \mathbb{T}_{IB}\boldsymbol{h}$$

is constant, when represented in $\mathcal{F}_I$.

When friction is neglected and g_i is the torque applied to the i–th wheel about its spin axis by an ideal electric motor (that is, disregarding electric motor and driver internal dynamics), one has [16]

$$\dot{h}_{r_i} = g_i - I_w\,\dot{\boldsymbol{\omega}}^T\hat{\boldsymbol{e}}_i \qquad [5]$$

where the torques g_i, $i = 1, 2$, represent the control inputs. As an alternative, it is possible to directly assume the vector $\dot{\boldsymbol{h}}$ as the control input for the design of the attitude control law, thus removing any argument on whether friction needs to be accounted for.

2.2 *Minimum attitude error with zero residual angular rate*

It is assumed that the desired attitude, $\mathcal{F}_D = \{O; \hat{\boldsymbol{E}}_1, \hat{\boldsymbol{E}}_2, \hat{\boldsymbol{E}}_3\}$, is fixed in the inertial frame, $\mathcal{F}_I$, hence it is possible to consider $\mathcal{F}_I \equiv \mathcal{F}_D = \{O; \hat{\boldsymbol{E}}_1, \hat{\boldsymbol{E}}_2, \hat{\boldsymbol{E}}_3\}$. The residual angular momentum is represented in $\mathcal{F}_I$ by the vector

$$\begin{aligned}\boldsymbol{h}_I &= H_0\hat{\boldsymbol{\eta}}_0 = H_0(\eta_1, \eta_2, \eta_3)^T \\ &= H_0(\cos\alpha\cos\beta, \sin\alpha\cos\beta, \sin\beta)^T\end{aligned}$$

where H_0 is its magnitude, and the direction of the unit vector $\hat{\boldsymbol{\eta}}$ is identified by means of its azimuth and elevation angles, α and β, respectively, as reported in Fig. 1.

In the presence of a residual angular momentum, it is no longer possible to achieve any arbitrary attitude at rest, provided that an admissible rest attitude must allow the two active reaction wheels to absorb the angular momentum. This, in turns, requires that the (inertially fixed) angular momentum lies on the plane identified by the (body-fixed) directions of the spin axes of the two active RW's. This is equivalent to require that the underactuated axis, $\hat{\boldsymbol{b}}$, is normal to $\boldsymbol{h}$. Hence, admissible directions at rest for $\hat{\boldsymbol{b}}$ lie on the plane Λ, normal to $\hat{\boldsymbol{\eta}}_0$.

If one represents the attitude of the spacecraft by means of the 3-1-3 sequence of Euler angles, namely precession Ψ, nutation Θ, and spin Φ, the components of the underactuated direction $\hat{\boldsymbol{b}} = \hat{\boldsymbol{e}}_3$ are given by

$$\hat{\boldsymbol{e}}_3 = (\sin\Theta\sin\Psi, -\sin\Theta\cos\Psi, \cos\Theta)^T$$

Hence, the direction of $\hat{\boldsymbol{b}}$ for an admissible attitude must satisfy the constraint

$$\boldsymbol{h}\cdot\hat{\boldsymbol{b}} = \sin\Theta(\eta_1\sin\Psi - \eta_2\cos\Psi) + \eta_3\cos\Theta = 0$$

This requires that

$$\tan\Theta = \frac{-\eta_3}{\eta_1\sin\Psi - \eta_2\cos\Psi} \qquad [6]$$

The inverse tangent function provides values of Θ in the interval $[-\pi/2, \pi/2]$. Provided that the nutation angle is defined in the interval $\Theta \in [0, \pi]$, when a negative value of Θ is obtained, which corresponds to angles in the interval $\Theta \in [-\pi/2, 0]$, an angle π is added. In the end, for any precession angle Ψ, it is possible to identify from Eq. [6] a value of the nutation angle which makes the underactuated direction normal to the residual angular momentum vector, thus resulting into an admissible attitude with zero residual angular rate. Among all admissible attitudes, such that $\boldsymbol{h}\cdot\hat{\boldsymbol{b}} = 0$, it is possible to identify that which results into the overall minimum attitude error.

Letting $\hat{\boldsymbol{a}}$ and φ be, respectively, the Euler eigenaxis and Euler eigenaxis rotation angle which drive the body frame $\mathcal{F}_B$ onto the desired target attitude, $\mathcal{F}_D$, and $\mathbb{T}_{BD}$ the coordinate transformation matrix from the target (and inertial) frame to the body frame, it is

$$\mathrm{trace}(\mathbb{T}_{BD}) = 1 + 2\cos\varphi$$

which clearly shows that the attitude error, associated to the amplitude of the Euler eigenaxis rotation, φ, is minimized when the trace of $\mathbb{T}_{BD}$ is maximized.

When expressed in terms of Euler angles for the 3-1-3 sequence, the trace of $\mathbb{T}_{BD}$ achieves the form

$$\mathrm{trace}(\mathbb{T}_{BD}) = (1 + \cos\Theta)\cos(\Phi + \Psi) + \cos\Theta$$

For a given value of Θ, $\mathrm{trace}(\mathbb{T}_{BD})$ is maximized for $\Phi + \Psi = 0$, that is, $\Phi = -\Psi$, in which case its value becomes

$$\mathrm{trace}(\mathbb{T}_{BD}) = 1 + 2\cos\Theta$$

Note that, in this condition, the attitude error φ coincides with the nutation angle, Θ. Hence, a global minimum for the attitude error is obtained when the spacecraft achieves the attitude with the minimum admissible nutation angle and a spin angle $\Phi = -\Psi$, equal in magnitude but opposite in sign to the precession angle.

In the framework of all admissible attitudes, the minimum value of the Θ is achieved when $\hat{\boldsymbol{e}}_3$ lies at the intersection of the plane Λ with the plane Γ, identified by the unit vectors $\hat{\boldsymbol{E}}_3$ and $\boldsymbol{h}$. In which case it is $\Theta \equiv \beta$. Note that, in such a case, the line of the nodes generated by the intersection of Γ with the plane Σ, identified by the directions of the unit vectors $\hat{\boldsymbol{E}}_1$ and $\hat{\boldsymbol{E}}_2$. The corresponding value of the precession angle is thus given by $\Psi = \alpha - \mathrm{sign}(\alpha)(\pi/2)$ (Fig. 1), where $\mathrm{sign}(\cdot)$ is the sign function which provides 1 when the argument is positive and -1 when negative.

Summarizing, the minimum error attitude at rest is achieved when (i) the precession angle is equal to $\Psi_m = \alpha - \text{sign}(\alpha)(\pi/2)$, $\Theta_m = \beta$, and, following the discussion reported above, the spin angle is $\Phi_m = -\Psi_m$. Note that, all this considered, the elevation of the angular momentum vector over the $\hat{\boldsymbol{E}}_1 - \hat{\boldsymbol{E}}_2$ plane directly provides the value of the minimum attitude error which can be achieved with zero angular velocity, in a rest-to-rest maneuver. When this angle is large, the resulting attitude error may result unacceptably high, also in the case in which the residual momentum is small in magnitude.

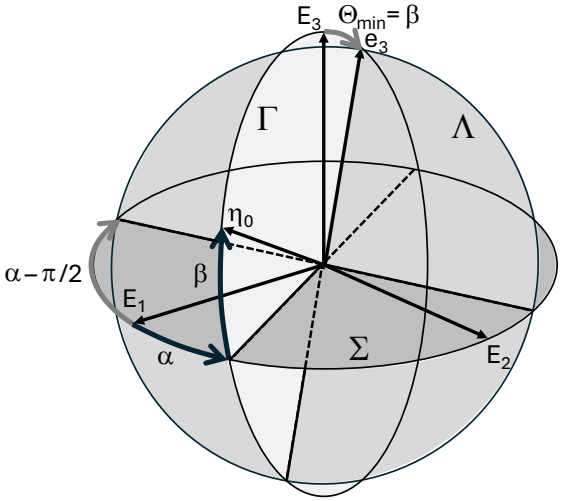

Fig. 1: Relevant unit vectors and angles for the minimum error attitude in the presence of a residual angular momentum.

2.3 *Spinning periodic solutions*

When $0 \leq \Theta \leq \Theta_m = \beta$, a component $h_3 = H_0 \sin(\beta - \Theta)$ of the angular momentum is projected along the direction $\hat{\boldsymbol{b}} = \hat{\boldsymbol{e}}_3$ of the failed wheel, whereas the remaining component $H_0 \cos(\beta - \Theta)$ is projected on the $\hat{e}_1$-$\hat{e}_2$ plane, where the active wheels can exchange angular momentum with the platform.

If nutation and precession angles are to be held constant, with $\Psi = \Psi_m$, it is $\dot{\Phi} = \omega_3$, the presence of a non-zero angular momentum component along $\hat{\boldsymbol{e}}_3$ implies that a non-zero angular velocity component is present around that axis, $\omega_3 = (H_0/J_3)\sin(\beta - \Theta)$. Hence, the spin angle will vary as $\Phi(t) = \Phi_m + \omega_3 t$, a condition which can be maintained if the angular momentum of the active reaction wheels with a spin axis parallel to $\hat{e}_1$ and $\hat{e}_2$, is varied periodically as $h_1 = H_0 \cos(\beta - \Theta)\cos(\Phi - \Phi^\star)$ and $h_2 = -H_0 \cos(\beta - \Theta)\sin(\Phi - \Phi^\star)$, respectively, where $\Phi^\star = \text{sign}(\alpha)(\pi/2)$.

Such a spin condition allows the platform to pass closer to the target attitude, than the minimum error attitude at rest determined above, but only for a limited amount of time, provided that during most of the rotation around $\hat{\boldsymbol{b}} = \hat{\boldsymbol{e}}_3$ the attitude error will become (possibly much) larger.

3. MPC controller

Consider a nonlinear time-invariant system governed by the following equation:

$$\dot{x}(t) = f(x(t), u(t)) \qquad [7]$$

where $x(t) \in \mathcal{X} \subseteq \mathbb{R}^{n_x}$ is the state vector at time $t \in \mathbb{R}$, $u(t) \in \mathcal{U} \subseteq \mathbb{R}^{n_u}$ is the input vector (where $\mathcal{U}$ is a convex, closed, and compact set, containing the origin in its interior), and $f(x, u)$ a sufficiently smooth function. The measurements of the state vector are sampled with period $T_S > 0$. At each sampling time $t = t_k$, a prediction of the system state $\hat{x}(t)$ over the time interval $[t_k, t_k + T_p]$ is performed, where $T_p \geq T_S$ is the prediction horizon.

The nonlinear MPC optimal control problem is formulated as follows.

$$\begin{aligned} &u^* = \arg\min_u J\big(x(t), u(t)\big) \\ &\text{subject to:} \\ &\dot{\hat{x}}(\tau) = f(\hat{x}(\tau), \hat{u}(\tau)), \;\; \hat{x}(t_k) = x(t_k), \\ &\hat{x}(\tau) \in \mathcal{X} \subseteq \mathbb{R}^{n_x}, \; \hat{u}(\tau) \in \mathcal{U} \subseteq \mathbb{R}^{n_u}, \\ &(x(\tau), u(\tau)) \in \mathcal{M} \subseteq \mathbf{R}^{n_x \times n_u} \;\; \forall \tau \in [t_k, t_k + T_p]. \end{aligned} \qquad [8]$$

Associating to each solution $\hat{x}$ of [8] the tracking error $\tilde{x}(\tau) = \hat{x}(\tau) - x_r$, we employ a performance index

$$\begin{aligned} J = \int_{t_k}^{t_k + T_p} \big(\|\tilde{x}(\tau)\|^2_{\mathbf{Q}} + \|\hat{u}(\tau)\|^2_{\mathbf{R}}\big)\, \mathrm{d}\tau + \\ + \|\tilde{x}(t_k + T_p)\|^2_{\mathbf{P}} \end{aligned} \qquad [9]$$

where $\mathbf{Q}, \mathbf{P} \succ 0 \in \mathbb{R}^{n_x \times n_x}$ and $\mathbf{R} \succ 0 \in \mathbb{R}^{n_u \times n_u}$ are suitable diagonal matrices to be designed. Note that, as usual for the MPC setting, the receding horizon strategy is employed. Hence, only the first sample of the optimal input signal is applied to the plant, while the 'tail' of the solution is discarded. The same procedure is repeated at each optimization step t_k.

3.1 *Implementation of NMPC to attitude control*

The NMPC controller is based on prediction of the system behavior along a finite time window. Such prediction is carried out by employing a model of the system dynamics. In this work, we use the same SC dynamics both for the NMPC prediction model and the plant, except for the SC inertia matrix $\boldsymbol{J}$ which, in the prediction model, is considered to be diagonal, i.e., the direction of RWs' spin axes are perfectly aligned with the SC principal axes of

inertia. This kind of situation is typical in real scenarios, where the knowledge of the SC inertia matrix is subject to uncertainty.

The NMPC prediction model consists of the Euler equation for the angular velocity evolution [4] (accounting also for the wheels dynamics [3]), as well as, the quaternion evolution [2]. In summary, the attitude model consists of a set of affine-in-the-input first-order differential equations where the state is $x \doteq [\boldsymbol{\omega}, q_0, \bar{\boldsymbol{q}}, \boldsymbol{h}]^T \in \mathbb{R}^{10}$ and the control input is $u \doteq [g_1, g_2]^T \in \mathbb{R}^2$; g_i is the torque applied to the i-th wheel about its spin axis by an electric motor. Note that, in this work, except for the angular momentum bias, no further external disturbances are accounted for.

Hence, the overall closed-loop system is defined by joining together [2] and [4], with $u^* = [g_1^*, g_2^*]^T$ computed as the solution of the optimal control problem [8]. In order to make the optimal control problem efficient from a numerical point of view, a finite pice-wise parametrization of the input signal u has been assumed, with changes of values at the nodes $\tau_1, ..., \tau_N \in [t_k, t_k + T_p]$ with $N \in \mathbb{N}$ being the number of nodes. In the following, we consider $N = 1$ (i.e. a constant input for every $\tau \in [t_k, t_k + T_p]$). The value $N = 1$ was chosen, since ensuring a satisfactory tracking/convergence performances, while guaranteeing a low computational burden of the optimization algorithm.

3.2 *System constraints*

Referring to [8], $\mathcal{X}$, $\mathcal{U}$, and $\mathcal{M}$ are set describing possible state, input, and mixed input-state constraints, respectively. For the application at hand, no limitation on the satellite rotation about its three axis is imposed, while a saturation on the RWs deliverable torques is taken into account. Nevertheless, the latter statement does not automatically imply that the full state remains unconstrained, since one has to take into account that the overall satellite dynamics accounts also for the RW angular momentum $\boldsymbol{h}$. In light of this, the state and the output are not bounded singularly, whereas the feasible set is a (linear, for the application at hand) polytope which takes both the input and the state as arguments. Whereby, the resulting scenario consist in a mixed input-state constraints set

$$\|\boldsymbol{g}\tau_{EM} - \boldsymbol{h}\|_\infty \leq 0.1\tau_{EM} \qquad [10]$$

where τ_{EM} is a scaling constant referred to the RW electric motor, and recalling that g_i and h_i are the control input and the angular momentum of the i-th wheel, respectively. Mathematically speaking, the set of admissible values of $\ell(x, u) \doteq \boldsymbol{g}\tau_{EM} - \boldsymbol{h}$ is the polytope

$$\mathcal{M} \doteq \big\{\ell(x,u) = \boldsymbol{g}\tau_{EM} - \boldsymbol{h} \in \mathbb{R}^{2\times 2} : \\ -0.1\tau_{EM} \leq g_i\tau_{EM} - h_i \leq 0.1\tau_{EM},\ i \in \{1,2\}\big\}. \qquad [11]$$

Hence, given the above definition in [11], within the NMPC algorithm, we do not impose any further saturation or constraints on the controlled input $\boldsymbol{g} \doteq [g_1, g_2]^T$.

4. Results

We consider the nominal satellite matrix of inertia $\boldsymbol{J} = \mathrm{diag}(3, 4, 5)$ kg m^2. Wheel inertia around the spin axis is assumed equal to $\mathbf{I}_w = 0.01$ kg m^2. Once data for the residual angular momentum vector represented in $\mathcal{F}_I$ are chosen, namely H_0, α, and β, a zero-angular rate minimum error attitude can be determined, according to the derivations reported in Subsection 2.2. In the following, we consider $H_0 = 0.005$ Nms, $\alpha = \beta = 10^\circ$.

In the framework of the simulation campaign, the following initial conditions are randomized:

- A pseudo-random initial attitude, according to the method devised in [17].
- Random initial values for h_1 and h_2, assuming a uniform probability density function over the range $h_{i,0} \in [-2H_0; 2H_0]$, $i = 1, 2$, thus generating the initial angular momentum vector for the wheels, $\boldsymbol{h}_r(t_0) = [h_{1,0}, h_{2,0}, 0]^\top$.

Hence, the initial values for the SC angular velocity components is thus given by $\boldsymbol{\omega}(t_0) = \boldsymbol{J}^{-1}[\mathbb{T}_{BD_0}\boldsymbol{h}_I - \boldsymbol{h}_r(t_0)]$, where $\mathbb{T}_{BD_0}$ is the coordinate transformation matrix for the initial random attitude.

4.1 *Case 1: Minimum attitude error with zero residual angular rate*

For the case where we steer the SC attitude to a rest condition with a minimum attitude error, we choose to control both the quaternion and the angular rate to the prescribed reference, as depicted in Section 2.2. Thus, referring to the cost function [9], the matrices $\mathbf{P}, \mathbf{Q} \in \mathbb{R}^{10\times 10}$ are built such that only the diagonal entries relevant to the quaternion and angular rate can have non-null values. By means of a trial-and-error procedure, the matrices are chosen as $\mathbf{P} = \mathrm{diag}(10^3, 700, 500, 700, 100, 100, 100, \mathbf{0}_{3\times 1})$, $\mathbf{Q} = \mathrm{diag}(7 \cdot 10^3, \mathbf{0}_{2\times 1}, 9 \cdot 10^5, 100, 100, 100, \mathbf{0}_{3\times 1})$, whereas $\mathbf{P}$ guarantees closed-loop convergence to an arbitrarily small, attractive, and invariant set, centered on the reference [14]. $\mathbf{Q}$ consists of a sort of a kinematic planning for the attitude maneuver. Indeed, the higher is the value

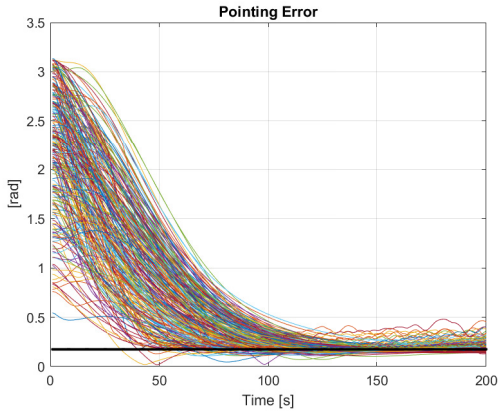

Fig. 2: Minimum pointing error at rest condition: SC pointing error evolution. The black line represents the theoretical minimum pointing error.

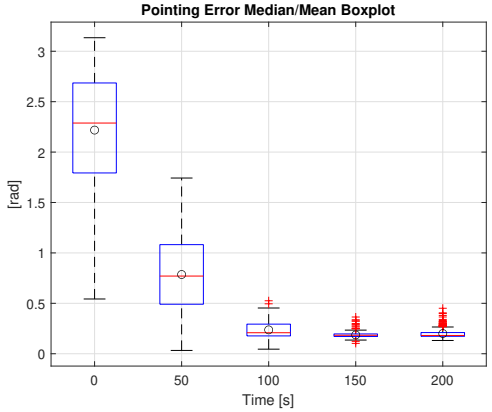

Fig. 3: Minimum pointing error at rest condition: SC pointing error boxplot.

of the diagonal entry of $\mathbf{Q}$, the faster is the convergence of the relevant state. Furthermore, we have $\mathbf{R} = \mathbf{I}_{3\times3}$, where $\mathbf{I}$ is the identity matrix. The controller works at 1 Hz, i.e. $T_S = 1$ s, while the prediction horizon is set as $T_p = 15T_S$. To conclude, the optimal control problem has been solved in a Matlab environment by means of the nonlinear optimization toolbox and employing the sequential quadratic programming iterative method. Finally, the Monte Carlo campaign consists of 250 simulated cases with randomized initial conditions spanning over a 200 s time window.

A plot of the variation of the resulting pointing error during the runs is shown in Fig. 2 where the black line represent the theoretical minimum pointing error achievable by the SC (i.e., $\beta = 10°$). In Fig. 4, we show the average value, inside the range between the maximum and the minimum pointing error, as well as the 3σ deviation, recorded at each time instant for the whole set of simulations. Figure 3 shows the statistical properties of the distribution of pointing errors between 0 and 200 s, every 50 s, in terms of average value, median, variance and range. In this latter figure, the central red line inside each box indicates the median, while the the black circle is the mean. The bottom and top edges of the box indicate the 25th and 75th percentiles, respectively. The whiskers extend to the most extreme data points (outliers excluded). Outliers, that is, cases which violates the calculated range of variation by more than 3σ, are plotted individually using a '+' marker symbol. Note that, as outcome of the Monte Carlo campaign, we obtain a dozen of outliers – at the end of the maneuver – over 250 cases.

NMPC delivers good convergence properties, despite the wide variation in initial error and residual initial angular momentum. In fact, as Monte Carlo output, the angular rate of SC (Fig. 5), and the control torques (the NMPC command in Figure 7 and the resulting RWs torques in Figure 6) are also displayed. It is evident that, together with a good tracking of the desired reference attitude, NMPC also guarantees satisfying performance in terms of residual angular rate, which, nevertheless, is not totally nullified. It is worth to note that the Monte Carlo campaign confirms the effectiveness of the proposed NMPC controller in finding a set of feasible rotations – despite an underactuated direction and an initial residual in terms of angular momentum – without any higher kinematic planning level. This is a remarkable property of NMPC: the capability to jointly carry out the two tasks of planning and control.

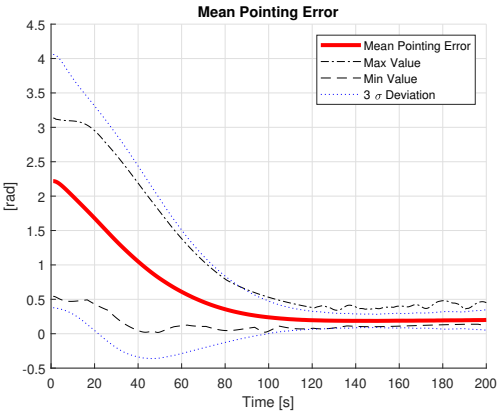

Fig. 4: Minimum pointing error at rest condition: In red the SC mean pointing error evolution, in dashed-dotted black line the minimum and maximum values (at each sampling step), in dotted blue the 3σ deviation with respect to the mean value at each sampling step.

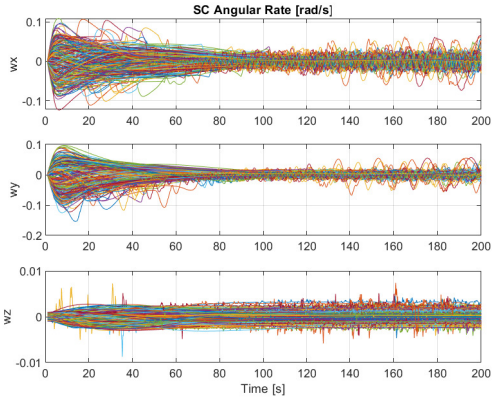

Fig. 5: Minimum pointing error at rest condition: SC angular rate evolution.

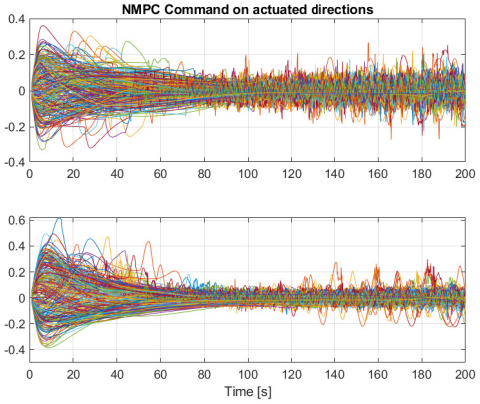

Fig. 7: Minimum pointing error at rest condition: NMPC command to the wheels.

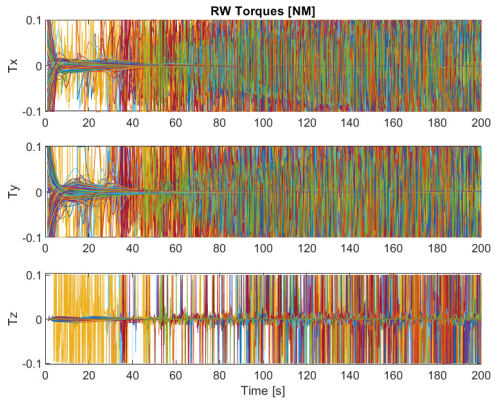

Fig. 6: Minimum pointing error at rest condition: Torques delivered by the RWs.

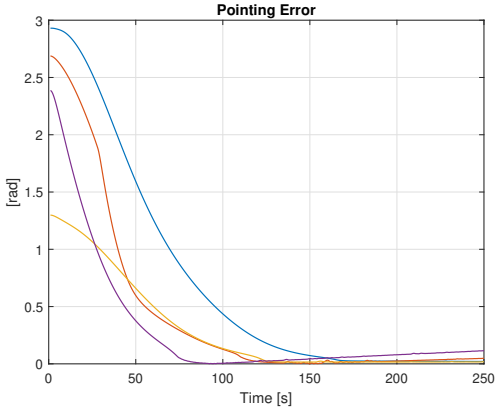

Fig. 8: Spinning periodic solution: SC pointing error evolution

4.2 *Case 2: spinning periodic solutions*

For the case of spinning periodic solution we limit the simulated cases to a few units, over a similar time scale of the first scenario presented. In contrast to the first simulated scenario, for the spinning periodic solution, we choose to also control the state of the first two RWs, according to the reference provided in Section 4.2.

Referring to the cost function [9], the matrices $\mathbf{P}, \mathbf{Q} \in \mathbb{R}^{10\times10}$ are chosen as $\mathbf{P} = \mathrm{diag}(10^3, 700, 500, 700, 100, 100, 10000, 50, 50, 0)$, $\mathbf{Q} = \mathrm{diag}(7 \cdot 10^3, \mathbf{0}_{2\times1}, 9 \cdot 10^5, 100, 100, 10000, 50, 50, 0)$. Furthermore, we have $\mathbf{R} = \mathbf{I}_{3\times3}$, where $\mathbf{I}$ is the identity matrix. The controller works at 1 Hz, i.e. $T_S = 1$ s, while the prediction horizon is set to $T_p = 15T_S$. As in the previous scenario. In the latter case, the simulations span a time window of 250 s. From 8 it is worth to notice how, by keeping a residual of angular rate on the SC axes, it is possible to reach – for a limited amount of time – the zero pointing error condition. On the other hand, ω_3 (see Fig. 9) is forced to keep a constant value in steady state, in order to allow the SC to periodically rotate towards the reference-pointing axis. Finally, torques delivered by RWs are plotted in Fig. 10, while the NMPC command in Fig. 11.

Finally, Figs. 10-11 the torques delivered by the RWs cluster, as well as, the relevant optimal input signal provided by the NMPC controller.

5. Conclusions

An underactuated spacecraft NMPC attitude controller is developed and presented in detail, which demonstrate the capability of efficiently managing an angular momentum bias, due to the residual effect of external perturbations. Stabilization performance have been demonstrated by means of an extensive simulation campaign by refer-

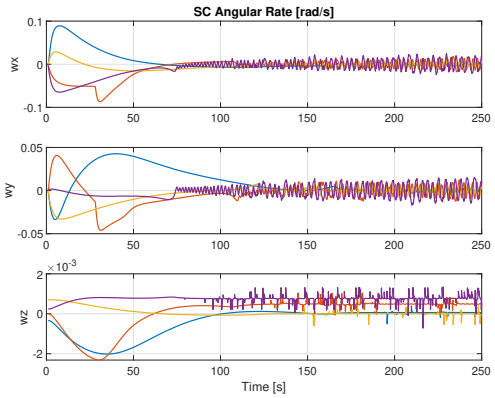

Fig. 9: Spinning periodic solution: SC angular rate evolution.

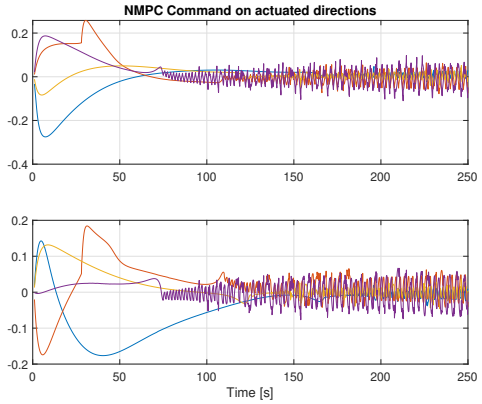

Fig. 11: Spinning periodic solution: NMPC command to the wheels.

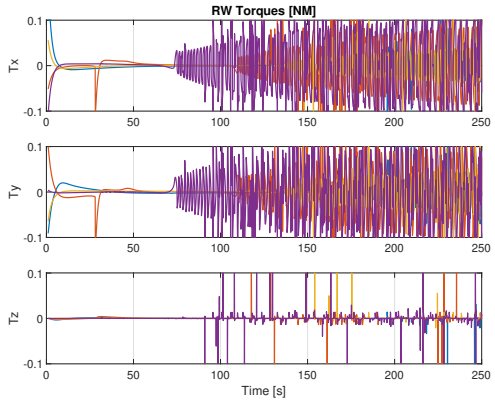

Fig. 10: Spinning periodic solution: Torques delivered by the RWs.

ring to a small satellite platform equipped with only two operative reaction wheels in two different scenarios: i) stabilization towaards a minimum pointing error at rest and ii) tracking a periodic spinning solution which allows for an almost zero attitude error, at some time during the rotation.

Simulations results confirm the effectiveness of the proposed NMPC controller in both aforementioned scenario, showing an excellent behavior in tracking the desired attitude, while guaranteeing a smooth manoeuvre and robustness against the residual initial angular momentum. Monte Carlo campaign prove how the NMPC controller is a suitable technology for this kind of attitude maneuvers, by autonomously identifying the set of feasible rotations - despite an underactuated direction - without any higher level kinematic planning while providing an optimal control action. Further work will be focused in employing different kind of SC actuators (e.g., magnetic torquers) and/or more advanced NMPC tools, including robust NMPC as well as and NMPC for reference tracking.

References

[1] G. Avanzini, F. Giulietti, E. Minisci, and F. Berardo, "Optimal rotation sequences in presence of constraints on admissible rotation axes," *Journal of Guidance, Control, and Dynamics*, vol. 34, no. 2, pp. 8554–563, 2011.

[2] G. Bucchioni and M. Innnocenti, "Rendezvous in cis-lunar space near rectilinear halo orbit: Dynamics and control issues," *Aerospace*, vol. 8, no. 3, p. 68, 2021.

[3] G. Avanzini, D. Zona, F. Giulietti, and A. Palmas, "Application of singular perturbation theory to space flight dynamics problems," *International Astrodynamics Conference (IAC)*, 2022.

[4] S. Vidano, M. Pagone, J. Grzymisch, V. Preda, and C. Novara, "Drag-free and attitude control system for the lisa space mission: An H_∞ constrained decoupling approach," *IEEE Transactions on Control Systems Technology*, pp. 1–15, 2024.

[5] J. Wertz, *Spacecraft attitude determination and control*. Dordrecht, The Netherlands: D. Reidel Publishing Company, 2nd ed., 1978.

[6] G. Avanzini, E. De Angelis, F. Giulietti, C. Novara, and M. Pagone, "Control of underactuated spacecraft by dynamic implementation of a sequence of feasible rotations," in *Proceedings of the 2023 AAS/AIAA Astrodynamics Specialist Conference*, 2023.

[7] C. Byrnes and A. Isidori, "On the attitude stabilization of a rigid spacecraft," *Automatica*, vol. 27, no. 199, pp. 87–95, 1991.

[8] A. Zavoli, G. Matteis, F. Giulietti, and G. Avanzini, "Single-axis pointing of an underactuated spacecraft with two reaction wheels," *Journal of Guidance, Control, and Dynamics*, vol. 40, no. 6, pp. 1465–1471, 2017.

[9] G. Avanzini, A. Zavoli, G. Matteis, and F. Giulietti, "Single axis pointing for underactuated spacecraft with a residual angular momentum," *Aerospace Science and Technology*, vol. 124, pp. 1–17, 2022.

[10] E. Camacho and C. Bordons, *Model Predictive Control*. London, UK: Springer, 2013.

[11] Ø. Hegrenæs, J. Gravdahl, and P. Tøndel, "Spacecraft attitude control using explicit model predictive control," *Automatica*, vol. 41, no. 12, pp. 2107–2114, 2005.

[12] J. C. Sanchez, R. Vazquez, J. D. Biggs, and F. Bernelli-Zazzera, "Orbit-attitude predictive control in the vicinity of asteroids with in situ gravity estimation," *Journal of Guidance, Control, and Dynamics*, vol. 45, no. 2, pp. 262–279, 2022.

[13] M. Mammarella, D. Lee, H. Park, E. Capello, M. Dentis, and G. Guglieri, "Attitude control of small spacecraft via tube-based model predictive control," *Journal of Spacecraft and Rockets*, vol. 56, no. 3, pp. 1–18, 2019.

[14] M. Pagone, M. Boggio, C. Novara, A. Proskurnikov, and G. C. Calafiore, "Continuous-time nonlinear model predictive control based on Pontryagin Minimum Principle and penalty functions," *International Journal of Control*, article in press, 2024.

[15] K. Wie, B, *Space Vehicle Dynamics and Control*. Reston, VA: American Institute of Aeronautics and Astronatics, Inc., 2nd ed., 2008.

[16] E. de Angelis, F. Giulietti, A. Ruiter, and G. Avanzini, "Spacecraft attitude control using magnetic and mechanical actuation," *Journal of Guidance, Control, and Dynamics*, vol. 39, no. 3, pp. 564–573, 2016.

[17] K. Shoemake, *Uniform random rotations*. New York: Academic Press, 1992.